PCP
PLANT & CELL PHYSIOLOGY

The Metabolic Signature of Biomass Formation in Barley

Mohammad R. Ghaffari[1,2], Fahimeh Shahinnia[2], Björn Usadel[3], Björn Junker[4], Falk Schreiber[5], Nese Sreenivasulu[6] and Mohammad R. Hajirezaei[2,*]

[1]Agricultural Biotechnology Research Institute of Iran (ABRII), Agricultural Research, Education and Extension Organization (AREO), Tehran, Iran
[2]Leibniz Institute of Plant Genetics and Crop Plant Research, Corrensstraße 3, D-06466 Gatersleben, Germany
[3]Institute of Botany, RWTH Aachen University, BioSC Germany and IBG-2 Plant Sciences, Forschungszentrum Jülich, D-52428 Jülich, Germany
[4]Institute of Pharmacy/Biosynthesis of Active Substances, Hoher Weg 8, Halle (Saale), Germany
[5]Monash University, Clayton Campus, Wellington Road, Clayton, VIC 3800, Australia
[6]International Rice Research Institute, DAPO Box 7777, Metro Manila, Philippines
*Corresponding author. E-mail, mohammad@ipk-gatersleben.de; Fax, +49-39482-5515.
(Received November 19, 2016; Accepted June 16, 2016)

Regular Paper

The network analysis of genome-wide transcriptome responses, metabolic signatures and enzymes' relationship to biomass formation has been studied in a diverse panel of 12 barley accessions during vegetative and reproductive stages. The primary metabolites and enzymes involved in central metabolism that determine the accumulation of shoot biomass at the vegetative stage of barley development are primarily being linked to sucrose accumulation and sucrose synthase activity. Interestingly, the metabolic and enzyme links which are strongly associated with biomass accumulation during reproductive stages are related to starch accumulation and tricarboxylic acid (TCA) cycle intermediates citrate, malate, *trans*-aconitate and isocitrate. Additional significant associations were also found for UDP glucose, ATP and the amino acids isoleucine, valine, glutamate and histidine during the reproductive stage. A network analysis resulted in a combined identification of metabolite and enzyme signatures indicative for grain weight accumulation that was correlated with the activity of ADP-glucose pyrophosphorylase (AGPase), a rate-limiting enzyme involved in starch biosynthesis, and with that of alanine amino transferase involved in the synthesis of storage proteins. We propose that the mechanism related to vegetative and reproductive biomass formation vs. seed biomass formation is being linked to distinct fluxes regulating sucrose, starch, sugars and amino acids as central resources. These distinct biomarkers can be used to engineer biomass production and grain weight in barley.

Keywords: Biomass • Central metabolism • *Hordeum vulgare* L • Metabolomics • Systems biology • Transcriptomics.

Abbreviations: MS, mass spectrometry; TCA, tricarboxylic acid. The complete list of abbreviations for metabolites, amino acids and enzymes is presented in Supplementary Table S2.

Introduction

Graminaceous plants including wheat (*Triticum aestivum* L.), rice (*Oryza sativa* L.), sorghum (*Sorghum bicolor* L.) and barley (*Hordeum vulgare* L.) deliver a major part of the food resources needed for human societies. Due to their constituents and their large acreage, the dual use of these plants as a future food source for human and animals and as biomass energy crops has attracted considerable attention (McLaren 2005). In particular, the composition of cell wall and storage carbohydrates differs markedly in cereals and other grass species from those in dicotyledonous plants. The cell wall of grasses contains more heteroxylan and less pectin or xyloglucan compared with the cell walls of other higher plants (Fincher 2009; reviewed in Burton and Fincher 2014). In addition, the major storage carbohydrate in cereals is fructan, and there is less starch which is the most common transitory storage compound in dicotyledonous plants. All these features and the importance of grasses as possible biomass energy crops make them feasible targets for a thorough identification of possible candidate genes determining biomass. Here, barley was used as a model crop that is a potential dual-use energy plant and exhibits a large genetic diversity (*Hordeum vulgare* L.) with different biomass performance and growth habit. In Europe, Germany in particular is one of the largest barley-producing countries (http://faostat.fao.org) and the largest producer and user of biomass fuel. Thus, barley can be used as a model crop plant due to its genetic resources, and its comparatively simpler genome from which knowledge can be transferred to other food crops where the straw could have a second use, e.g. wheat or sugar sorghum (sorghum). One way to improve yield and composition is by investigating the metabolic status of a plant.

This is because the metabolic status of a plant reflects the balance between growth and assimilate storage (Meyer et al. 2007, Aharoni and Brandizzi 2012). A more predictive understanding of the many and complex inter-relationships determining the constitution of the metabolome is becoming possible with the elaboration of technology platforms which permit the simultaneous analysis of large numbers of metabolites (Fernie and Schauer 2009). Associations between growth rate and a subset of metabolites have been determined in *Arabidopsis thaliana* by performing interecotype comparisons (Meyer et al. 2007, Sulpice et al. 2013). Genetically determined variation in metabolite content can be generated by changes in the activity of one or more enzymes, allowing for the means to link changes in metabolite content to defined allelic variation

Plant Cell Physiol. 57(9): 1943–1960 (2016) doi:10.1093/pcp/pcw117, Advance Access publication on 7 July 2016, available online at www.pcp.oxfordjournals.org

(Keurentjes et al. 2008). In maize, the level of activity of certain enzymes associated with central carbon or nitrogen metabolism has been correlated with grain weight accumulation (Zhang et al. 2010), and similarly that of photosynthetic enzymes has been correlated with biomass accumulation in *A. thaliana* (Sulpice et al. 2010).

Global transcriptomic analysis has uncovered a wealth of knowledge concerning the diurnal variation in gene transcription (Covington et al. 2008). It has also aided the identification of numerous transcription factors responsible for the regulation of genes encoding key enzymes in carbon and nitrogen metabolism (Sreenivasulu and Wobus 2013). In addition, the identification of various metabolites involved in central metabolism that includes assimilation, respiration, transport and differentiation processes deciphered the importance of metabolites for a possible improvement of plant growth and development (Lisec et al. 2008, Fernie and Schauer 2009, Wen et al. 2015). By integrating transcriptomic- and metabolomic-based data, a number of potential targets has been identified as the means to manipulate fruit composition in tomato (Carrari et al. 2006) and similarly to recognize *A. thaliana* genes important for biomass formation during its vegetative phase (Meyer et al. 2007). As yet, such a comprehensive study that includes different omics tools combined with various developmental stages has not been attempted to analyze the genetic basis of biomass accumulation in the cereals.

The present research aims to determine whether the rate of biomass accumulation shown by the barley plant could be correlated with its metabolic composition, to identify which metabolites, enzymes and/or genes are important in directing the plant to accumulate specific storage compounds, and to explore which metabolic pathways may present feasible targets for modification with the aim of increasing biomass and/or grain yield.

To fulfill these aims, we used a comprehensive and integrative approach investigating the metabolic-, enzymatic- and transcript-related traits among contrasting barley genotypes at three different developmental stages. We identified metabolic and/or transcript signatures highly indicative for biomass formation and elucidated the connection between metabolites, enzymes and transcripts in central metabolism. The profiles of metabolites, enzymes and genes were analyzed to comprise key metabolic pathways or processes during the formation of shoot and seed biomass in barley as a cereal model plant.

Results

Phenotypic variation of shoot biomass

In order to identify barley lines contrasting in their shoot biomass for further experiments, shoot biomass was determined at three different developmental stages of a micropanel of 12 contrasting barley lines which showed a maximum genotypic variation for shoot biomass evaluated in a pre-experiment under field trial conditions (**Supplementary Table S1**). The accumulated biomass of the panel of 12 barley entries is shown in **Supplementary Fig. S1**. The performance of the entries varied significantly ($P < 0.01$) with respect to shoot biomass at the vegetative, reproductive and grain ripening stages. The best performing entries were HOR216, cv. Scarlett, HOR4730, HOR3909 and HOR7410, while the poorest was S42IL107. The differences were consistently exhibited at each growth stage, except in the case of S42L107 (**Supplementary Fig. S1**).

In the following sections, we then profile metabolites and enzyme activities in detail in this panel at three stages, namely at the vegetative tillering stage, at the reproductive stage and at anthesis. In each stage, we determine whether certain metabolites are indicative of biomass at the same stage. In addition we build correlation networks to unravel interactions between metabolites potentially indirectly driving biomass.

Metabolites and enzymes linked to shoot biomass accumulation at the vegetative stage (tillering, BBCH29)

To elucidate which primary metabolites and enzymes involved in central metabolism might determine the accumulation of shoot biomass at the vegetative stage of barley development, metabolite profiling and enzyme activity measurements were carried out. The Pearson correlation analysis outcomes are listed in **Supplementary Table S3** and illustrated graphically in **Fig. 1**. Large sections of metabolite and enzyme groups are in light to dark brown colors reflecting the association regions of metabolic traits with similar chemical structures such as glucose-6-phosphate (Glc6P) and fructose-6-phosphate (Fru6P). The Calvin cycle enzymes plastidic fructose-1,6-bisphosphatase (pFBPase) and plastidic glyceraldehyde-3-phosphate dehydrogenase (pGAPDH) displayed 13 connections, the glycolytic enzyme phosphofructokinase (PFK) six connections and the tricarboxylic acid (TCA) cycle enzyme isocitrate dehydrogenase (ICDH) seven connections. A total of 168 direct links were identified between metabolite content and enzyme activity ($P < 0.05$); however, there were seven connections noted between an enzyme's activity and the amount of its substrate or product present. An example of such a positive link was between the glycolysis enzyme phosphofructokinase and its substrate fructose-6-phosphate.

Among the metabolites associated with shoot biomass accumulation were sucrose (Suc) (+0.80), pyruvate (Pyr) (+0.60), fructose-6-phosphate, glucose-1-phosphate (Glc1P) (−0.62), UDP glucose (UDPGlc) (−0.75), citrate (Cit) (−0.57), isocitrate (Isocit) (−0.57), glutamate (Glu) (−0.71), lysine (Lys) (−0.59), glycine (Gly) (−0.62), valine (Val) (−0.59) and serine (Ser) (−0.65) (**Fig. 1**, marked in dark brown).

Seven enzymes were significantly correlated with shoot biomass accumulation: these were the two sucrose-degrading enzymes sucrose synthase (Susy) (+0.80) and cell wall invertase (CWInv) (−0.61), the two Calvin cycle enzymes plastidic fructose-1,6-bisphosphatase (−0.65) and glyceraldehyde-3-phosphate dehydrogenase (−0.64), the two glycolytic enzymes phosphofructokinase (−0.75) and pyruvate kinase (PK) (−0.75), and the nitrogen metabolism enzymes phosphoenolpyruvate carboxylase (PEPC) (−0.69) and aspartate aminotransferase (AspAT) (−0.58) (**Fig. 1**, marked in medium dark brown).

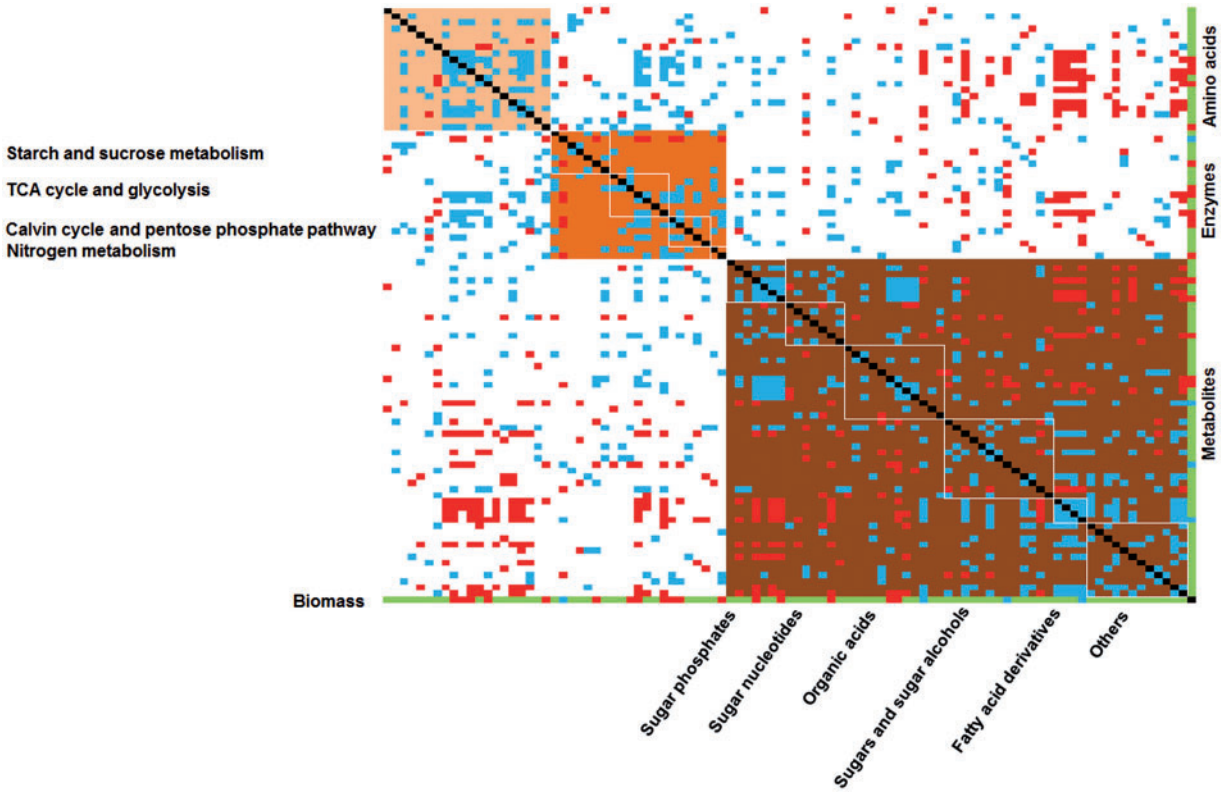

Fig. 1 A heat map illustrating correlations between metabolite content and biomass at the vegetative stage. The colored squares indicate a correlation of either enzyme activities (medium brown) or metabolites (light and dark brown) with biomass (green). Only significant (P-value < 0.05) correlations have been presented. Positive and negative correlations are colored, respectively, in red and blue. The full names and abbreviations of the enzymes and metabolites are presented in **Supplementary Tables S2** and **S3**.

Network correlation analysis of different metabolites and enzymes in shoots at the reproductive stage (anthesis, BBCH65)

To find specific correlations between metabolites and enzyme activities in barley shoots at the reproductive developmental stage, network correlation analysis was performed. The results highlighted 658 positive (shown as blue edged in **Supplementary Fig. S2A**) and 68 negative (red-edged) correlations between metabolite contents and enzyme activities in the flag leaf post-anthesis; the full set is listed in **Supplementary Table S4**. The largest connections concerned the TCA cycle intermediates citrate, malate (Mal), *trans*-aconitate (Tacnt) and isocitrate, UDP glucose, ATP and the amino acids isoleucine (Ile), valine, glutamate and histidine (His) (**Supplementary Fig. S2A**). When the correlation network analysis was applied to the enzymes involved in various metabolic pathways, the strongest enzyme/enzyme correlation proved to be between isocitrate dehydrogenase (TCA cycle) and aspartate aminotransferase (nitrogen metabolism), and between the two sucrose metabolism enzymes sucrose synthase and phosphoglucomutase (PGM) with ADP-glucose pyrophosphorylase (AGPase), the key enzyme in starch synthesis (**Supplementary Fig. S2B**; **Supplementary Table S4**). Aspartate aminotransferase and alanine aminotransferase (AlaAT) were strongly correlated with isocitrate dehydrogenase and phosphoenolpyruvate, while sucrose synthase was negatively correlated with ADP-glucose pyrophosphorylase, phosphoglucoisomerase (PGI), phosphoglucomutase, plastidic fructose-1,6-bisphosphatase and cytosolic aldolase (cAldolase) (**Supplementary Fig. S2B**, marked in red). The amino acids asparagine (Asn), glutamate and glutamine (Gln) were strongly correlated with the enzyme alanine aminotransferase (**Supplementary Fig. S2A**). Other notable correlations were found for citrate and galactose (Gal) that correlated with the enzyme glutamine oxoglutarate aminotransferase (GOGAT) involved in nitrogen metabolism (**Supplementary Fig. S2B**).

Metabolites and enzymes required for shoot biomass accumulation at anthesis (BBCH65)

The anthesis phase is characterized by a rearrangement of metabolic pathways. Thus, specific metabolites and enzymes required for shoot accumulation at the anthesis stage were identified. A set of 24 metabolites was identified as being associated with shoot biomass accumulation around the time of anthesis (**Fig. 2A**; **Supplementary Table S4**). These included the TCA cycle intermediates malate (r-value +0.74), succinate (Succ) (+0.67), *trans*-aconitate (Tacnt) (+0.70), *cis*-aconitate (Cacnt) (+0.57), fumarate (Fum) (+0.64) and isocitrate (+0.72) and the amino acids valine (+0.72), isoleucine (Ile) (+0.67), methionine (Met) (+0.66) and aspartate (Asp)

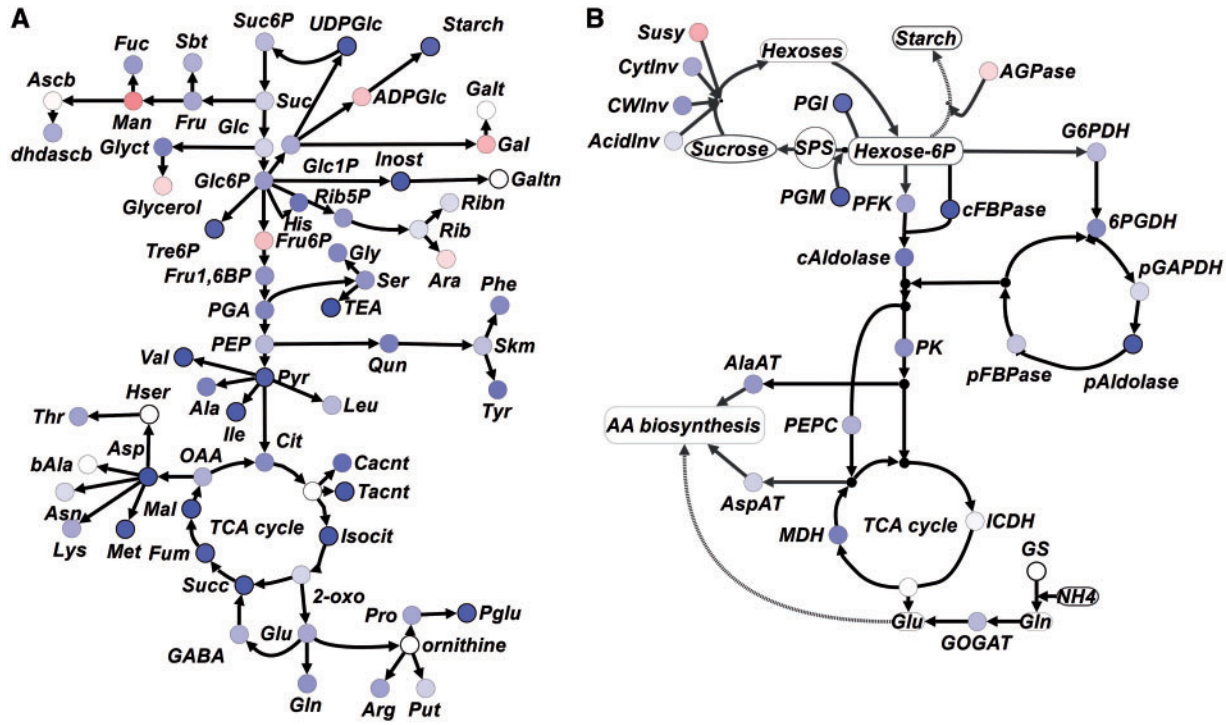

Fig. 2 Metabolite contents and enzyme activities significantly correlated with shoot biomass accumulation at the reproductive stage. Positive (red) and negative (blue) correlations with shoot biomass for (A) metabolite content and (B) enzyme activity. The darker color shows the stronger correlation. The full names and abbreviations of the enzymes and metabolites are presented in **Supplementary Tables S2** and **S3**.

(+0.78) (**Fig. 2A**, lower panel marked in blue). Of the 22 enzymes identified, the activity of four, namely phosphoglucoisomerase (+0.58), phosphoglucomutase (+0.64), plastidic aldolase (pAldolase) (+0.68) and cytoplasmic fructose-1, 6-bisphosphatase (cFBPase) (+0.69), was positively correlated with shoot biomass (**Fig. 2B**, upper panel marked in blue; **Supplementary Table S4**).

Differential transcription of genes determining biomass formation in the shoot during the reproductive stage

As we had determined that some general metabolic–enzymatic signatures were related to biomass, we wanted to explore this further based on the expression signatures in barley shoots at the reproductive stage. To address this aim, we selected the two most contrasting entries, namely HOR216 (highest biomass accumulator; **Supplementary Table S2**) and S42IL107 (lowest biomass accumulator; **Supplementary Table S2**) and performed detailed transcriptome analysis. These were subjected to a transcriptomic comparison based on the Agilent 56K microarray, focusing on genes involved in carbohydrate, energy and nitrogen metabolism (**Supplementary Fig. S1**). In the leaves, this analysis revealed the differential transcription of 1,512 genes (1,278 higher in HOR216 and 234 in S42IL107); of these, 131 and 177, respectively, were associated with primary metabolism (**Supplementary Fig. S3A**; **Supplementary Table S5**). Genes prominent in the light reaction and the Calvin cycle were significantly over-represented (**Fig. 3**, right panel; **Supplementary Table S5**). The latter included genes encoding transketolase (TK), plastidic fructose-1,6-bisphosphatase, triose-phosphate isomerase (TPI), sedoheptulose bisphosphatase (SBP) and phosphoglycerate kinase (PGK), which were all more abundantly transcribed in HOR216, and fructose 1,6-bisphosphate aldolase and ribose 5-phosphate isomerase (RPI), which were both less abundantly transcribed (**Fig. 3**). Genes associated with carbohydrate (CHO) metabolism were also significantly over-represented (**Fig. 3**). Large fold differences in transcript abundance were recorded for genes associated with aromatic amino acid metabolism: 19 such genes were transcribed more abundantly in HOR216 by up to 2.6-fold, while the two less abundantly transcribed genes differed in abundance by up to 7.0-fold (**Fig. 3**, upper panel, left side).

The relationship between shoot biomass, transcript abundance and enzyme activity

Here, a correlation analysis was performed to find the relationship between identified transcripts and the measured enzyme activities. Applying a stringent criterion (r-value $>+0.70$ or <-0.70), a subset of 933 transcripts was selected to correlate transcript abundance with enzyme activity (22 enzymes) and shoot biomass at the reproductive stage. The combined network revealed a large number of positive correlations (507 connections) and a lower number of negative ones (262 connections). The activity of phosphoglucoisomerase, alanine aminotransferase and ADP-glucose pyrophosphorylase was in each case highly correlated with its encoding gene's transcript

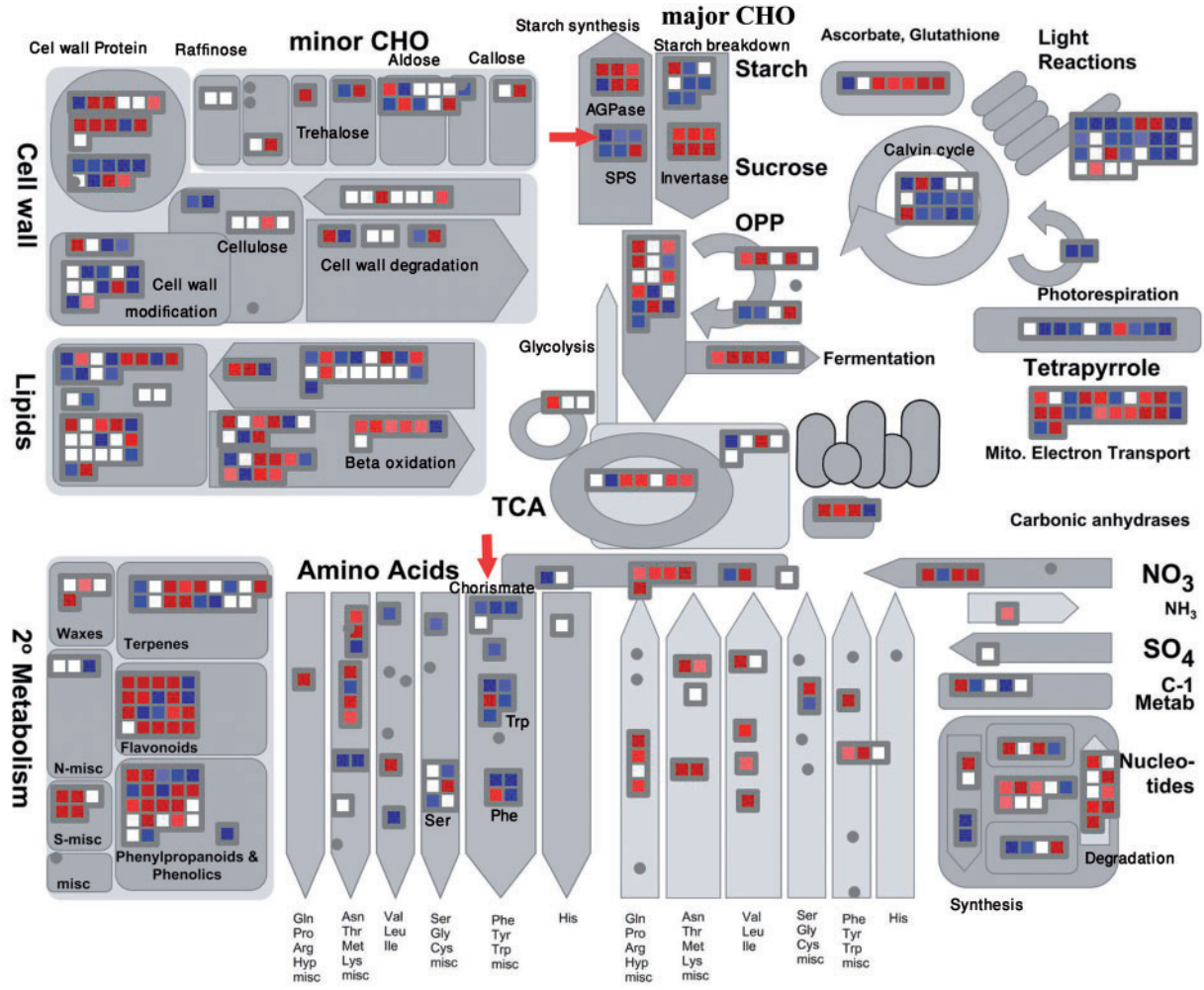

Fig. 3 Schematic representation of differentially transcribed transcripts in the flag leaf of HOR216 (high biomass producer) vs. S42II107 (low biomass producer). The red and dark blue colors represent at least a 4-fold higher transcript abundance and are colored, respectively, in red and blue. The over-represented transcripts are indicated with red arrows.

abundance (**Supplementary Table S6**). However, only seven genes were transcribed in accordance with the activity of ADP-glucose pyrophosphorylase, 6-phosphogluconate dehydrogenase (6PGDH), alanine aminotransferase, plastidic glyceraldehyde-3-phosphate dehydrogenase, cytoplasmic fructose-1,6-bisphosphatase, phosphoglucoisomerase and phosphoglucomutase activity (**Table 1**).

The relationship between metabolite content, enzyme activity and grain weight

In order to find out what metabolites or enzymes within central metabolism are being linked as biomarkers for grain weight as a final biomass, the relationship between metabolites, enzymes and grain weight was analyzed. In the young barley grain (15 d post-anthesis), the strongest metabolite–metabolite connections were between the structurally similar monosaccharides fructose (Fru) and glucose (Glc) (*r*-value +0.95), two fatty acid-derived compounds hexadecanoic acid (Hxda) and octadecanoic acid (Odca) (+0.97), glucose-6-phosphate and fructose-6-phosphate (+0.76), two TCA cycle intermediates succinate and malate (−0.83), and starch synthesis compounds ADP-glucose (ADPGlc) and glucose-1-phosphate (+0.95) (**Supplementary Fig. S4A**; **Supplementary Table S7**). The levels of ascorbate (Ascb), ATP and sucrose were also prominent (43 connections) in the network (**Supplementary Fig. S4A**). Valine and leucine (Leu) were the most connected amino acids (**Supplementary Fig. S4A**). The strongest correlation between metabolites and amino acids involved succinate, isocitrate, citrate and *cis*-aconitate with glutamate (**Supplementary Fig. S4A**). Significant correlations were also detected between metabolites associated with distinct pathways: for instance, fructose and glucose content was negatively correlated with that of the metabolite oxaloacetic acid (OAA) and the polyamine putrescine (Put) (**Supplementary Fig. S4A**). With respect to the activity of the set of 22 enzymes, the most highly connected were cytosolic invertase (CytInv) and acid invertase (AcidInv) (sucrose metabolism), along with phosphoglucoisomerase and cytosolic fructose-1,6-bisphosphatase (glycolysis) (**Supplementary Fig. S4B**). A weaker connection was detected for sucrose synthase and phosphoenolpyruvate carboxylase (**Supplementary Table S7**). The analysis implied that

Table 1 Pearson correlation analysis illustrating the relationship between transcript abundance and enzyme activity for enzymes involved in central metabolism with shoot biomass accumulation during the reproductive stage

Metabolic pathway	Enzyme	Barley ID	Gene annotation	*r*-value	*P*-value
Starch metabolism	AGPase	HVSMEi0002I05r2_at	ADP-glucose pyrophosphorylase	−0.91	4.00E-05
Pentose phosphate pathway	6PGDH	Contig5852_at	6-Phosphogluconate dehydrogenase	+0.71	9.00E-03
Nitrogen metabolism	AlaAT	35_29082	Alanine aminotransferase	+0.78	6.00E-03
Calvin cycle	pGAPDH	Contig3720_s_at	Plastidic glyceraldehyde 3-phosphate dehydrogenase	+0.73	6.00E-03
Glycolysis	cFBPase	35_29225	Cytosolic fructose 1,6-bisphosphatase	+0.77	4.00E-03
Sucrose metabolism	PGI	S0000800188A02F1_at	Phosphoglucoisomerase	+0.79	2.00E-03
	PGM	Contig1650_at	Phosphoglucomutase	+0.83	8.00E-04

Significant positive and negative associations are indicated.

the activity of enzymes assigned to sucrose metabolism (including phosphoglucomutase, phosphoglucoisomerase and cytosolic and acid invertases) was correlated strongly with those of the two nitrogen metabolism enzymes glutamine oxoglutarate aminotransferase and alanine aminotransferase, and that of the starch metabolism enzyme ADP-glucose pyrophosphorylase (**Supplementary Fig. S4B**).

Correlations between metabolite content and grain weight

To evaluate which metabolites and/or enzymes might have a positive or negative effect on the composition and final weight of barley grains, the content of metabolites and the activity of enzymes in seeds were correlated with grain weight (**Fig. 4A, B**). The contents of fumarate (*r*-value −0.72), malate (−0.57), *cis*-aconitate (−0.60), citrate (−0.76) and isocitrate (−0.70) were all negatively correlated, while that of succinate (+0.77) was positively correlated with grain weight. Other correlations involved grain weight with the content of isoleucine (+0.70), tyrosine (Tyr) (+0.71), phenylalanine (Phe) (+0.70) and tryptophan (Trp) (+0.73), while that of aspartate (−0.65) and glutamate (−0.76) was negatively correlated. The content of each of the sugars sucrose (−0.72), ascorbate (−0.84), inositol (Inost) (−0.81) and ribose-5-phosphate (Rib5P) (−0.67) was also negatively correlated with grain weight. Among the metabolites, ATP (+0.85) and UDP (+0.66), along with UDP glucose (+0.61) contents were all positively correlated. Grain weight was positively correlated with the activity of several enzymes: ADP-glucose pyrophosphorylase (+0.66), phosphoglucomutase (+0.65), phosphoglucoisomerase (+0.63), phosphofructokinase (+0.57) and alanine aminotransferase (+0.74), but negatively with cytosolic invertase (−0.71).

Identification of differentially transcribed genes affecting grain weight at the reproductive stage

We next investigated which individual genes correlate with grain weight by performing a transcriptome analysis on barley grains at the reproductive stage. The correlation analysis between the identified genes and grain weight revealed at the level of transcription a total of 5,067 genes that were differentially abundant between HOR216 and S42IL107 (2,194 higher in the former and 2,873 higher in the latter). Among these, 207 and 129, respectively, represented genes involved in central metabolism (**Supplementary Fig. S3B**; **Supplementary Table S8**). The functional enrichment analysis revealed 12 gene clusters for carbohydrate and amino acid metabolism, particularly featuring sucrose and starch synthesis and starch degradation (**Fig. 5**; **Supplementary Table S8**). Among the 10 genes involved in starch breakdown were those encoding starch phosphorylase (a 2.0-fold difference), triose phosphate translocator (2.0-fold), β-amylase (15-fold) and starch-binding domain (3.0-fold). Sucrose phosphate synthase (SPS) transcripts were also over-represented (**Fig. 5**).

Combined network of transcripts, enzymes activities and grain weight

The regulation of the genes at the transcription level does not necessarily go along with a regulation on the protein level as proteins can be regulated by post-translational modification. We therefore performed correlation analysis between transcripts, enzymes and grain weight to evaluate the genes and proteins being regulated at both levels and which have a profound effect on the grain yield. The combination network incorporating enzyme activity, transcript abundance and grain weight was constructed based on a 933 transcript subset, involving mainly genes associated with energy, carbohydrate and amino acid metabolism. The network featured 1,098 associations, of which 613 were negative and 484 positive (**Supplementary Table S9**). Among the enzymes, glutamine oxoglutarate aminotransferase, cytosolic aldolase and phosphoglucoisomerase were the ones associated with the highest connectivity (130, 125 and 113 connections, respectively). In contrast, malate dehydrogenase (MDH) had only one connection and phosphofructokinase had three. The activity of phosphoglucoisomerase and glucose-6-phosphate dehydrogenase (G6PDH) was positively correlated with the abundance of phosphofructokinase (35_6515) and the *threonine aldolase* (HVSMEg0009L14r2_at) transcript. Similarly the activity of ADP-glucose pyrophosphorylase and alanine aminotransferase was correlated with the abundance of transcript for genes encoding hydrolase (35_31565) and Cyt *b*5 (Contig1920_at). Of the 933 transcripts, only seven genes were transcribed in accordance with their activity of ADP-glucose pyrophosphorylase, sucrose synthase, glucose-6-phosphate dehydrogenase,

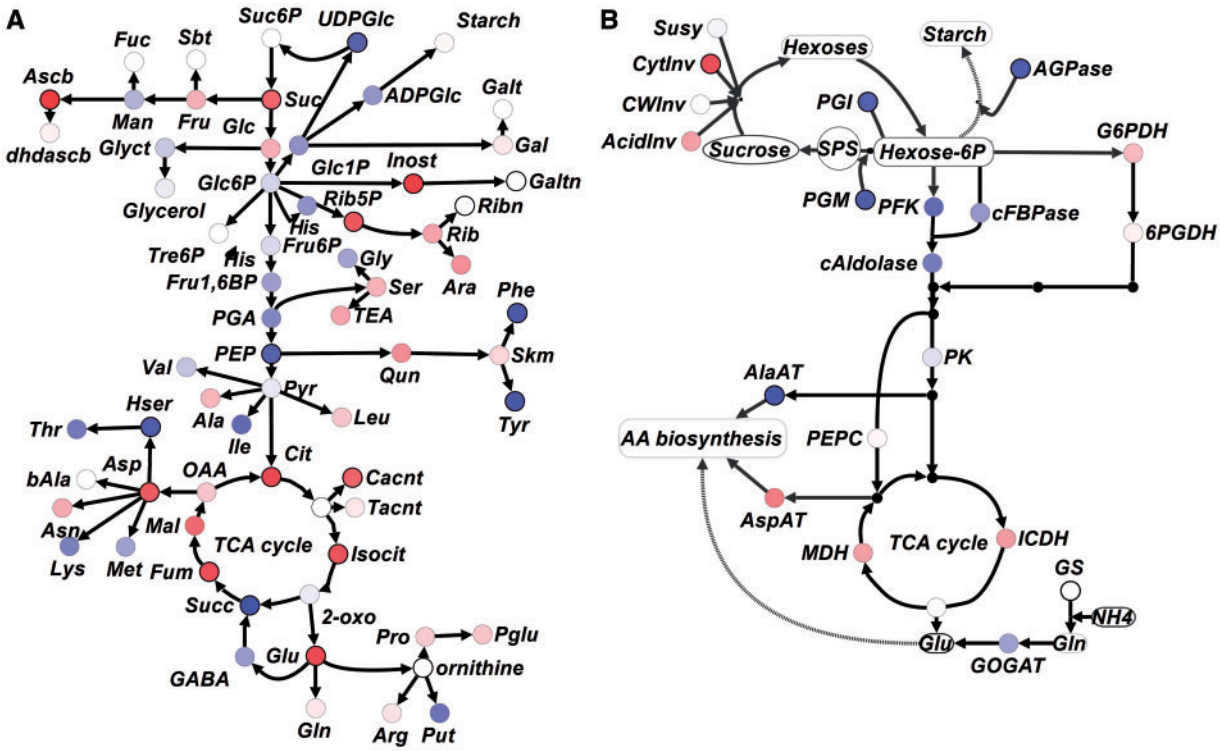

Fig. 4 (A) Metabolite contents and (B) enzyme activities significantly correlated with grain weight. Positive and negative correlations involving metabolites are colored, respectively, red and blue. Highly significant correlations are shown in darker colors. Further details are presented in **Supplementary Table S6**.

cytosolic aldolase, pyruvate kinase, isocitrate dehydrogenase and 6-phosphogluconate dehydrogenase (6PGDH) (**Table 2**).

Identification of differentially transcribed genes affecting cell wall composition at the reproductive stage in shoots and grains

In order to identify the genes involved in other metabolic pathways rather than primary metabolism, we evaluated the differentially expressed genes crucial for cell wall biosynthesis in shoots and grains of barley at the reproductive stage. Cell wall biosynthesis is a specific feature for cereals differing from that of non-gramineous plants and therefore an important target for biomass improvement.

The functional enrichment analysis revealed a gene cluster for cell wall metabolism, particularly featuring modification, cellulose and hemicellulose synthesis and cell wall proteins (**Table 4**). Among the genes involved in cell wall modification, endoxylanglucan transferase, some expansins and xyloglucan endotransglycolyse showed a reverse effect on biomass in shoots and grains with significant positive or negative correlation (**Table 4**).

Discussion

Compared with the major effort devoted by breeding programs to the development and implementation of markers linked to genes, trait-based biomarkers have been largely neglected. There have already been attempts to define the metabolomic, genetic and proteomic basis of shoot biomass in the model plant *A. thaliana* (Meyer et al. 2007, Sulpice et al. 2010, Bollina et al. 2011) and in crop plants to investigate the growth in tomato fruits (Carrari et al. 2006), the metabolite distribution in flag leaves of wheat grown in the field and which experienced terminal drought stress (Hill et al. 2013) and the leaf metabolites in a diverse maize inbred population (Riedelsheimer et al. 2012). In the present study, barley was used as a crop plant and the biomass accumulation was correlated with different traits including the metabolite composition, enzyme activity and transcripts at various developmental stages.

Metabolic traits correlated with shoot biomass accumulation during the vegetative stage

In the present study, many connections were revealed between metabolite levels and vegetative growth (**Fig. 1**). Some of these matched those identified in the *A. thaliana* rosette leaf (Sulpice et al. 2010) and the tomato fruit (Carrari et al. 2006). Some strong correlations were established between the contents of sucrose (the major output of photosynthesis), certain amino acids and glycolytic metabolites (**Fig. 1**). The metabolic network also featured negative relationships between metabolites involved in glycerophospholipid synthesis, fatty acid-derived metabolites, sugar nucleotides and sugar phosphates; this suggested that the biochemical regulation of biosynthetic routes

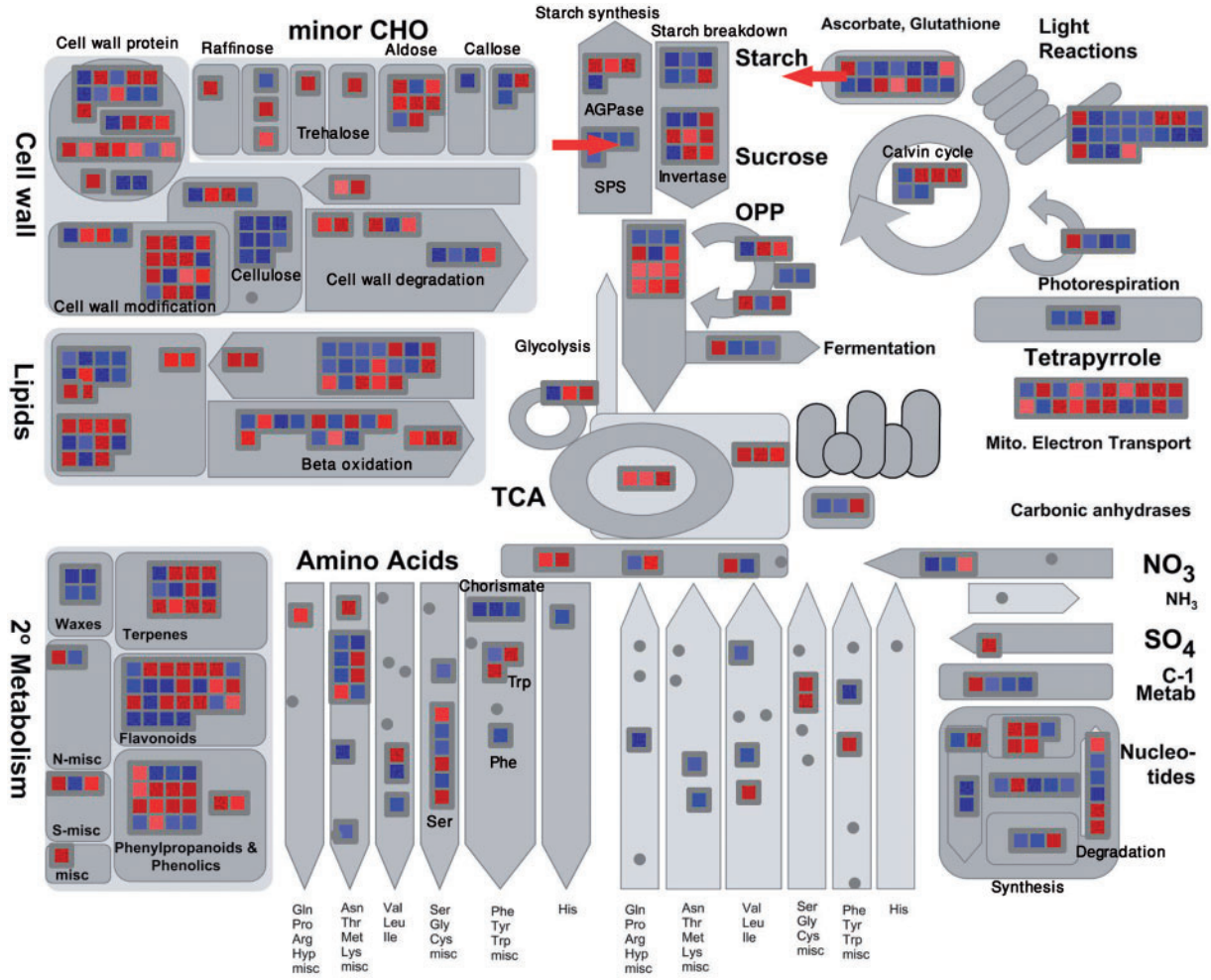

Fig. 5 Schematic representation of differentially transcribed genes in the grain of HOR216 vs. S42Il107. The red and dark blue colors represent an at least a 4-fold higher transcript abundance and are colored, respectively, red and blue. The over-represented transcripts are indicated with red arrows.

Table 2 Pearson correlation analysis illustrating the relationship between transcript abundance and enzyme activity for enzymes involved in central metabolism with grain weight

Metabolic pathway	Enzyme	Barley ID	Gene annotation	*r*-value	*P*-value
Starch metabolism	AGPase	35_4669	ADP-glucose pyrophosphorylase	−0.75	4.00E-03
Pentose phosphate pathway	6PGDH	35_806	6-Phosphogluconate dehydrogenase	+0.78	3.00E-03
	G6PDH	35_24090	Glucose-6-phosphate dehydrogenase	+0.75	7.00E-03
Sucrose metabolism	Susy	35_14485	Sucrose synthase	−0.74	8.00E-03
Glycolysis	cAldolase	35_14090	Cytosolic aldolase	−0.75	1.00E-03
	PK	35_15327	Pyruvate kinase	+0.74	6.00E-03
TCA cycle	ICDH	35_16234	Isocitrate dehydrogenase	+0.71	8.00E-03

Significant positive and negative associations are indicated.

drives the abundance of these intermediates in opposite directions as the site of carbon for the synthesis of building blocks for biomass production (Fig. 1). The observed strong co-regulation of certain metabolites, despite their being involved in distinct pathways in the leaf, implies that the modification of certain metabolic routes such as photosynthesis may have weight for determination of the end-product of related pathways. The correlation network associated with central metabolism featured positive connectivity between glycolysis, the TCA cycle, the Calvin cycle and sucrose metabolism (Fig. 1). The strong co-ordination of enzyme activity suggests that the more effective strategy for the plant to drive flux towards a specific end-product would be to co-regulate several enzymes within a pathway, rather than to rely on the effect of a single

Table 3 Pearson rank correlation coefficient between biomass accumulation and metabolite contents at various developmental stages of barley

	Negative		Positive
$p < 0.01$			
$p < 0.05$			

Metabolic traits	Vegetative stage total shoot biomass	Reproductive stage total shoot biomass	Reproductive stage total seed weight
PFK	−0.75		0.60
PK	−0.75		
pFBPase	−0.75		−0.60
pGAPDH	−0.60		
CWInv	−0.60		
PEPC	−0.60		
AspAT	−0.60		
AGPase			0.70
Susy	0.80		
AlaAT			0.70
CytInv			−0.70
PGM		0.60	0.60
PGI		0.60	0.60
cFBPase		0.70	
pAldolase		0.70	0.70
PEP			0.60
Glc1P	−0.65		
Fru6P	−0.60		
Cit	−0.60		−0.75
Isocit	−0.60	0.70	−0.70
Pyr	0.60	0.60	
Benza	0.60		
Suc	0.80		−0.60
Fum		0.60	−0.75
Mal		0.70	−0.60
Cacnt		0.60	−0.60
Succ		0.70	0.80
Tacnt		0.70	
Rib5P			−0.70
Tre6P		0.60	
UDP			0.65
ATP			0.80
UDPGlc	0.75	0.65	0.60
Pglu		0.70	
TEA		0.75	
Starch		0.60	
Hxda		0.70	
Inost		0.70	−0.80
Ascb			−0.80
Hser			0.70
Tdca		0.60	
Gly	−0.60		
Lys	−0.60		
Val	−0.60	0.70	

(continued)

Table 3 Continued

	Negative		Positive
$p < 0.01$			
$p < 0.05$			
Metabolic traits	**Vegetative stage total shoot biomass**	**Reproductive stage total shoot biomass**	**Reproductive stage total seed weight**
Met		0.70	
Ile		0.70	0.60
Tyr			0.70
Asp		0.80	0.65
Phe			0.70
Glu	−0.70		−0.75
Ser	−0.70		

Correlations at $P < 0.01$ and $P < 0.05$ are indicated by, respectively, dark and light red (negative correlations), and blue (positive correlations). The full set of correlations is provided in **Supplementary Tables S3** and **S4**.

enzyme. Metabolic modeling in *A. thaliana* has suggested that the modification of a single enzyme's activity can have a frequent but small effect on pathway flux (Zhu et al. 2007). Here, the enzymes from the same metabolic pathway showed a similar correlation pattern within and with other enzymes of different metabolic sectors (**Fig. 1**). As an example, enzymes associated with starch and with sucrose metabolism were co-regulated along with those involved in glycolysis and nitrogen metabolism.

Most of the correlations between metabolite content and enzyme activity were in the positive rather than in the negative direction (**Fig. 1**), consistent with prior expectation. Reducing the abundance of the sucrose synthase transcript (and hence the level of sucrose synthase activity) in the potato tuber has been shown to compromise starch synthesis (Zrenner et al. 1995). Positive correlations between metabolite level and enzyme activity, or between the levels of substrate and end-product present, have been established in both the tomato fruit (Steinhauser et al. 2010) and the grapevine berry (Dai et al. 2013). Here, most of the positive connections involved invertases and their products glucose and fructose (**Fig. 1**), a finding which contrasts with the performance of glasshouse-grown tomato, in which substrate/product contents were negatively correlated with one another (Steinhauser et al. 2010). The implication is that the metabolic network in barley is strongly affected by the plant's growing environment as well as by its developmental stage. The high frequency of positive correlations between enzyme substrates and products are first confined to irreversible biochemical reactions, secondly are dependent on the level of substrates (Sulpice et al. 2010) and finally reflect flux changes (Kacser and Burns 1973).

Enzyme activity and metabolite content in central metabolism are strongly correlated with shoot biomass accumulation

The network correlation analysis revealed that a number of central metabolism-associated metabolites and enzymes are strongly correlated with shoot biomass accumulation (**Fig. 1**). Sucrose is the predominant assimilate, serving not only as an energy source but also as a precursor of cellulose (Kirst et al. 2004). Sucrose is the substrate for sucrose synthase, an enzyme intimately involved in carbon partitioning in growing tissue. There was a strong correlation between sucrose synthase activity and shoot biomass at the reproductive stage, and a positive correlation between its activity and sucrose synthase transcript abundance; the conclusion is that sucrose synthase must act as a critical regulator for the partitioning of sucrose (**Supplementary Fig. S5**). In poplar, the transcription level of sucrose synthase was shown to be positively correlated with both cellulose synthesis and wood production (Hertzberg et al. 2001, Coleman et al. 2009). Similarly in wheat, sucrose synthase activity promotes cell wall polysaccharide production (Xue et al. 2008), while in tobacco it is positively correlated with biomass accumulation (Coleman et al. 2010). Consistently, in carrot, reducing sucrose synthase activity results in the development of smaller and fewer leaves (Tang and Sturm 1999), while in potato the effect is to reduce the tubers' content of both soluble sugar and starch (Zrenner et al. 1995). It is reasonable to suppose, therefore, that increasing sucrose synthase activity would enhance biomass accumulation in barley. This association between sucrose synthase activity and shoot biomass accumulation implies that it could be used predictively for the selection of high biomass producers, an important property for a bioenergy crop. The strong association between the content of UDP glucose, fructose-6-phosphate, glucose-1-phosphate and the activity of plastidic fructose-1,6-bisphosphatase and plastidic glyceraldehyde-3-phosphate dehydrogenase suggests a link between sucrose/starch synthesis and cell wall formation and the oxidative pentose phosphate pathway, which provides substrates for the synthesis of nucleic acids, lignin, polyphenol and amino acids, as well as for glycolysis.

Aspartate aminotransferase is a key enzyme for biomass production downstream of glycolysis and catalyzes the reversible reaction of 2-oxoglutarate, glutamate, aspartate and oxaloacetic acid produced by the TCA cycle, thereby tightly linking nitrogen assimilation with carbon metabolism. In the present study, the amino acid glutamate significantly correlated with shoot biomass accumulation, confirming the pivotal role of aspartate aminotransferase and glutamate in ammonium

Table 4 Pearson correlation analysis illustrating the relationship between transcript abundance for genes involved in cell wall metabolism with shoot (A: positive or B: negative) or grain (C: positive or D: negative) biomass

Trait	Barley ID	Mapman Gene Ontology	Gene	Correlation	*P*-value	Regulation	*P*-value (ANOVA)
Shoot biomass	A						
	35_18221	cell wall.pectin esterases	Acetyl esterase	+0.66	4.47E-02	Up	4.51E-02
	35_1073	cell wall.modification	Expansin A1	+0.68	3.97E-02	Up	4.18E-02
	35_9980	cell wall.modification	Expansin A10	+0.70	3.48E-02	Up	1.02E-02
	35_3043	cell wall.modification	Expansin like A2	+0.74	2.55E-02	Up	1.45E-02
	35_15358	cell wall.modification	Endoxyloglucan transferase A4	+0.86	1.22E-02	Up	1.46E-02
	B						
	35_1915	cell wall.precursor synthesis	Phosphomannomutase	−0.68	3.99E-02	Down	2.38E-02
	35_1537	cell wall.modification	Xyloglucan endotransglycosylase	−0.79	2.14E-02	Down	1.69E-02
Seed biomass	C						
	35_16574	cell wall.degradation	Cellulase	+0.69	2.34E-02	Down	3.86E-03
	35_8010	cell wall.degradation	endo-1,4-beta-glucanase	+0.88	1.38E-03	Down	2.90E-04
	35_22838	cell wall.pectin*esterases	Pectin methylesterase inhibitor superfamily	+0.75	1.10E-02	Down	6.20E-04
	35_14730	cell wall.cell wall proteins	Extensin family protein	+0.71	1.97E-02	Down	5.54E-04
	35_12759	cell wall.cellulose synthesis	Phytochelatin synthetase	+0.87	1.70E-03	Up	1.07E-09
	35_23609	cell wall.hemicellulose synthesis	Xyloglucan xylosyltransferase 5	+0.73	1.53E-02	Down	6.19E-04
	35_7907	cell wall.hemicellulose synthesis	AGP-galactosyltransferase 2	+0.73	1.53E-02	Down	1.51E-02
	35_3627	cell wall.hemicellulose synthesis	Fucosyltransferase 1	+0.68	2.58E-02	Up	3.44E-07
	35_10351	cell wall.modification	Expansin A14	+0.74	1.25E-02	Down	6.73E-03
	35_32047	cell wall.modification	Xyloglucan endotransglycosylase related 2	+0.78	7.49E-03	Down	3.07E-05
	35_11437	cell wall.modification	Expansin A8	+0.71	1.95E-02	Down	5.40E-04
	35_30696	cell wall.modification	Expansin A3	+0.91	8.07E-04	Down	1.31E-02
	35_3043	cell wall.modification	Expansin-LIKE A2	+0.88	1.54E-03	Down	2.05E-06
	D						
	35_28455	cell wall.precursor synthesis	UDP-xylose synthase 4	−0.91	8.66E-04	Down	1.71E-02
	35_9778	cell wall.cell wall proteins	Fasciclin-like arabinogalactan-protein 2 (Fla 2)	−0.79	6.57E-03	Up	3.14E-03
	35_1068	cell wall.degradation	Rsponsive to dessication 22	−0.77	8.95E-03	Up	1.18E-02
	35_18361	cell wall.pectin*esterases	Pectinacetylesterase family protein	−0.95	3.07E-04	Up	7.73E-03
	35_4496	cell wall.cellulose synthesis	Cellulase synthase 4	−0.86	2.38E-03	Up	4.70E-05
	35_12604	cell wall.pectin*esterases	Pectinesterase	−0.85	2.54E-03	Up	1.23E-03
	35_14895	cell wall.cell wall proteins	Proline rich protein 4	−0.86	2.21E-03	Up	3.70E-03
	35_14898	cell wall.cell wall proteins	Proline-rich family protein	−0.86	2.38E-03	Up	4.37E-03
	35_20775	cell wall.cellulose synthesis	Cellulose synthase 8, CESA8	−0.70	2.17E-02	Up	3.42E-07
	35_26740	cell wall.cellulose synthesis	Cellulose synthase	−0.91	8.89E-04	Up	5.29E-03
	35_10017	cell wall.cellulose synthesis	Cellulose synthase like A9	−0.88	1.54E-03	Up	1.20E-02
	35_25803	cell wall.hemicellulose synthesis	Golgi-localized hydroxyproline-*O*-galactosyltransferase	−0.74	1.35E-02	Down	1.85E-02
	35_20413	cell wall.modification	Expansin B3	−0.75	1.14E-02	Down	5.89E-03
	35_15359	cell wall.modification	Endosyloglucan transferase A4	−0.68	2.74E-02	Up	3.16E-02
	35_1072	cell wall.modification	Expansin A11	−0.69	2.26E-02	Up	3.02E-04
	35_18219	cell wall.modification	Expansin B2	−0.95	3.07E-04	Up	4.90E-03
	35_499	cell wall.modification	Xyloglucan endotransglycosylase 6	−0.68	2.71E-02	Up	2.44E-04
	35_3579	cell wall.modification	Expansin B4	−0.90	8.92E-04	Up	2.06E-02
	35_177	cell wall.modification	Xyloglucan endotransglycosylase 3	−0.79	7.21E-03	Up	3.96E-03

Significant positive and negative associations are indicated.

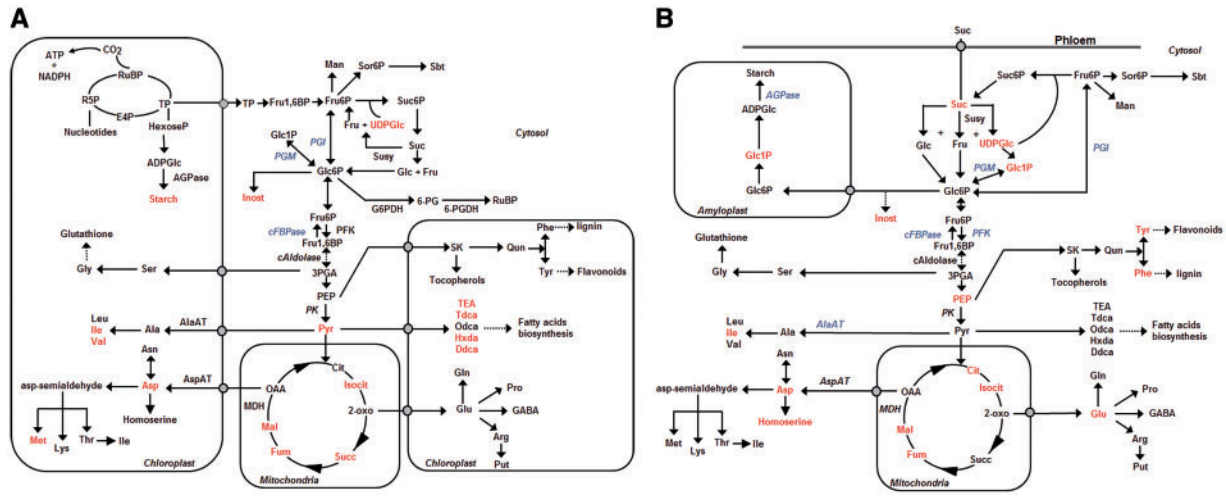

Fig. 6 Schematic representation of metabolites putatively involved in biomass formation during the reproductive stage in (A) the barley flag leaf and (B) the barley grain. The network correlation analysis identified a connection between biomass accumulation and central metabolism. Full names and the abbreviation of enzymes and metabolites are given in **Supplementary Table S2**. Metabolites associated with biomass accumulation are marked in red, and enzymes in blue.

assimilation and thereby in growth and development (Stitt et al. 2002). Another enzyme highlighted here was phosphoenolpyruvate carboxylase, which catalyzes the formation of oxaloacetate from phosphoenolpyruvate (PEP). Phosphoenolpyruvate carboxylase is branched to glycolysis to replenish TCA cycle intermediates, thereby providing precursors for amino acid synthesis. Strong associations between citrate and isocitrate content and the activity of pyruvate kinase and phosphofructokinase were also detected.

The predictive power of metabolite, enzyme and transcript assays for biomass accumulation during the reproductive stage

Studies in *A. thaliana* have established the potential of certain metabolite, enzyme and transcript assays as markers of biomass formation (Lisec et al. 2008, Sulpice et al. 2010, Riedelsheimer et al. 2012). The current data set was therefore used to test whether the same or different assays would be appropriate in barley. In the flag leaf, many of the transcripts which differed in abundance between the pair of contrasting barley entries could be associated with the activity of enzymes involved in either light reactions, the Calvin cycle, ATP synthesis or carbohydrate metabolism (**Fig. 3**). Transcripts of the genes encoding ribulose-1,5-bisphosphate carboxylase/oxygenase (Rubisco) were particularly prominent, followed by those encoding sedoheptulose-1,6-phosphatase and plastidic fructose-1,6-bisphosphatase. The latter two enzymes are involved in the regeneration of ribulose-1,6-bisphosphate, which is the immediate precursor for Rubisco (Harrison et al. 1997). A high abundance of transcripts encoding sedoheptulose 1,6-phosphatase and plastidic fructose-1,6-bisphosphatase in tobacco has been associated with an enhanced rate of photosynthesis and the potential to accumulate dry matter (Miyagawa et al. 2001). The cytoplasmic fructose-1,6-bisphosphatase and sucrose phosphate synthase are jointly responsible for the regulation of sucrose synthesis in the cytosol; the former catalyzes the conversion of fructose-1,6-bisphosphate (Fru1,6BP) to fructose-6-phosphate, which in turn is a precursor in the sucrose synthesis pathway. A mutant line of *Flaveria linearis* unable to produce cytoplasmic fructose-1,6-bisphosphatase is compromised with respect to both the partitioning of carbon into sucrose and its growth (Sharkey et al. 1992). A decreased activity of cytoplasmic fructose-1,6-bisphosphatase also reduces the level of phosphorylated intermediates and the ratio of cofactors such as ATP and ADP. Transgenic *A. thaliana* plants overexpressing genes encoding cytoplasmic fructose-1,6-bisphosphatase and a triose phosphate/phosphate translocator exhibit an increased photosynthetic activity and enhanced growth (Cho et al. 2012). The cytoplasmic fructose-1,6-bisphosphatase reaction product, along with UDP glucose, is used by sucrose phosphate synthase to produce UDP and sucrose-6-phosphate (Suc6P); the compound represents a substrate for sucrose phosphate phosphatase (SPP) to form sucrose. The present data showed that in barley, increasing cytoplasmic fructose-1,6-bisphosphatase and sucrose phosphate synthase activity can accelerate photosynthetic activity and consequently improve the partitioning of fixed carbon into sucrose in the leaf, thereby supporting reproductive development (Micallef et al. 1995). Previous investigations showed that maximal sucrose phosphate synthase activity in barley leaves correlated with high rates of in vivo sucrose biosynthesis, and a decrease in the sucrose phosphate synthase activity of barley leaf extracts upon dark phase was accompanied by a decrease of sucrose synthesis (Sicher and Kremer 1984). Thus, increasing the efficiency of the photosynthetic activity of the plant and hence the assimilate production are both key to maximizing plant biomass.

The starch content of the leaf appears to be a useful indicator for the growth rate (**Fig. 6A**). *Arabidopsis thaliana* mutants deficient with respect to either the synthesis or breakdown of starch are compromised in their growth (Stettler et al. 2009),

while starch also acts as a growth regulator in plants grown under long days (Sulpice et al. 2009). While the positive correlations were established between starch content and shoot biomass observed in barley in the present study (**Table 3**; **Supplementary Table S4**), the negative correlations were recorded between starch and rosette fresh weight in *A. thaliana* (Sulpice et al. 2009). These results imply that these correlations are strongly dependent on the species, the growing conditions and the plant developmental stage. The present network analysis involving enzyme activities and transcript abundances also revealed a significant association between the activity of ADP-glucose pyrophosphorylase (a key starch synthesis enzyme) and the transcript encoding ADP-glucose pyrophosphorylase in the shoot during the reproductive stage (**Supplementary Table S9**). In Arabidopsis and most vascular plants, starch as the primary product of photosynthesis plays an important role in the diurnal cycle of carbohydrate turnover in the leaf. The starch produced during the day provides a carbon source for leaf growth during the night as photosynthesis does not take place (Stitt and Zeeman 2012, Lloyd and Kossmann 2015). The photoassimilate partitioning into transitory starch varies among species, being about half for Arabidopsis (Streb and Zeeman 2012). In contrast to Arabidopsis, fructans are the major storage carbohydrate in wheat, barley, rye and oat (Pollock and Cairns 1991). However, starch is also accumulated in barley to a lesser extent and is mobilized during the night, but it would be delayed if the leaf sucrose level is higher, suggesting an important regulatory mechanism that differs from that of Arabidopsis (Gordon et al. 1980). A further contrast to Arabidopsis is that some cereals possess two genes which encode small subunits of ADP-glucose pyrophosphorylase of which the expression of one isoform in barley (*Hv.AGP.S1*) is regulated by alternative splicing. Additionally, one isoform is localized in the cytosol in endosperm while another, responsible for more than 90% of the total activity of ADP-glucose pyrophosphorylase, is localized in the chloroplasts. Extensive studies of the genes involved in starch synthesis and degradation have been carried out in both Arabidopsis and barley (reviewed in Orzechowski 2008, and references herein).

The content of trehalose-6-phosphate (Tre6P), an internal regulatory metabolite controlling the utilization of sucrose and the synthesis of starch (Paul et al. 2008), was highly correlated with biomass (**Fig. 2**). Trehalose-6-phosphate regulates starch synthesis by increasing the activity of ADP-glucose pyrophosphorylase (Wingler et al. 2000), at the same time acting as a signal to increase both carbon availability and nitrogen remobilization (Schluepmann et al. 2004, O'Hara et al. 2012). The activities of phosphoglucomutase, phosphoglucoisomerase and cytoplasmic fructose-1,6-bisphosphatase were all positively correlated with their encoding transcripts, implying a co-regulation of these enzymes at both the transcriptional and protein levels (**Supplementary Table S9**).

Metabolite content, enzyme activity and transcript abundance interact closely with grain weight

During the grain-filling period, storage products rapidly accumulate. The process involves the concerted action of many metabolites, which serve either as signals or as the precursors for storage or structural compounds. Sucrose was the metabolite most clearly associated with the accumulation of grain weight. Many genes were up-regulated in the grain, most prominently those encoding products involved in sucrose and starch metabolism (**Fig. 5**). The link between endosperm development and sucrose synthesis has been well documented (Hennen-Bierwagen et al. 2013) and underlines the major contribution made by sucrose phosphate synthase and sucrose phosphate phosphatase to grain development (Bihmidine et al. 2013). An overview of the metabolites (red) and enzymes (blue) within central metabolism which are being linked as biomarkers for grain weight is given in **Fig. 6B**. As the content of sucrose was strongly correlated with that of starch, it is clear that starch synthesis relies on the breakdown of sucrose catalyzed by sucrose synthase: these products are used for the synthesis of either starch (glucose) (Bihmidine et al. 2013, Hennen-Bierwagen et al. 2013) or UDP glucose (Xu et al. 2011). In contrast to the positive correlation of sucrose synthase, activity of invertases, the other sucrose-hydrolyzing enzymes, was negatively correlated to grain weight, supporting the suggestion that, in the developing grain, invertase activity is channeled into developmental processes during early seed development rather than into grain filling (Borisjuk et al. 2004).

The activity of alanine aminotransferase, an enzyme important for the synthesis of storage proteins, was also found to be highly correlated with grain weight. The heterologous transcription of barley alanine aminotransferase in rice has been associated with a marked improvement in nitrogen use efficiency (Beatty et al. 2009), which supports the suggestion that the manipulation of alanine aminotransferase expression may have a major impact on crop productivity (Ridley 2010). Glutamine oxoglutarate aminotransferase, another enzyme involved in nitrogen assimilation during grain development and in the production of glutamate required for the synthesis of many amino acids, also showed a high correlation with the transcript abundance at the reproductive stage. It has been shown that the overexpression of glutamine oxoglutarate aminotransferase in rice can markedly increase productivity (Yamaya et al. 2002). Other noteworthy correlations between metabolite content and grain weight involved specific amino acids, which are required for the production of storage and other proteins (Lawlor 2002).

Cell wall-related enzymes correlated with biomass during the reproductive stage

The main objective of the present work was the identification of genes and metabolites related to primary metabolism and biomass. However, due to remarkable differences in cell wall composition between barley and non-gramineous plants, a close search for possible candidate genes revealed that indeed some specific genes such as acetyl esterase, expansins, xyloglucan endotransglycosylases and endoxyloglucan transferases showed a strong correlation with biomass at the reproductive stage (**Table 4**). Xyloglucan endotransglycosylase (XET) has been shown to be involved in the elongation process in

maize roots and in plant growth by either synthesizing xyloglucan polymers into the cell wall or reversibly loosening the cellulose–xyloglucan network (De Silva et al. 1994). The genes predicted here play an important role in the cell wall of cereals as cellulose and heteroxylan are the most abundant polysaccharides in various barley tissues compared with Arabidopsis and other non-gramineous plants (Fincher 2009; reviewed in Burton and Fincher 2014). Thus, the identified genes might be used to modify the cell wall structure in different barley tissues to study their individual role in the mechanism and control of plant cell expansion, differentiation and maturation. Improvement of cell wall properties in barley would enhance the resistance property, e.g. of the leaves and/or the cell wall loosening of grains, for a better germination or digestion (Nishitani 1997).

Conclusion

A summary of the deduced metabolite and enzyme signatures potentially linked to biomass formation in the leaf and/or grain weight resulted in identification of various biomarkers as rate-limiting steps in central metabolism (**Table 3**). Some are only informative at a specific developmental stage, such as Susy activity in the early developmental stage, and glycolysis and TCA cycle intermediates being linked to biomass during the reproductive stage. The UDP glucose metabolite was found to be a central important hub of central metabolism prominently identified to have a stronger association with biomass in the vegetative and reproductive stage as well for grain weight. Together with ATP, ADP-glucose pyrophosphorylase (AGPase) activity from starch biosynthesis and alanine amino transferase (AlaAT) activity involved in synthesis of storage proteins were identified as rate-limiting steps in grain weight formation. Overall, the analysis has confirmed that metabolic responses related to the accumulation of biomass varies in a developmental stage-specific manner and in many cases in a tissue-specific manner as well.

Materials and Methods

Selection of accessions, growth conditions and sampling

Barley (*Hordeum vulgare* L.) accession lines used in this study were obtained from the gene bank of the Institute of Plant Genetics and Crop Plant Research (IPK), Gatersleben, and kindly donated by Professor Klaus Pillen, the University of Halle-Wittenberg (**Supplementary Table S1**). Seeds of spring barley were germinated separately in pots in a climate-controlled growth chamber for 2 weeks. The temperature was 12°C at night and 15°C during the day with a 12 h/12 h light/dark cycle. Then, seedlings were transferred in the field and planted in a completely randomized design (CRD) with a split plot arrangement (3.40 m × 1.20 m) and with five replications in the growing season of 2013 under in vivo conditions. The average growth temperature was 16.8°C. Samples were harvested at three different developmental stages according to the Biologische Bundesanstalt, Bundessortenamt und CHemische Industrie (BBCH) scale for crop plants (Lancashire et al. 1991) including vegetative (BBCH29, end of tillering: maximum number of tillers detectable; the harvested sample was tiller leaves), reproductive (BBCH65, end of flowering: all spikelet's have completed flowering but some dehydrated anthers may remain; the harvested sample was flag leaves and seeds) and ripening stages (BBCH92, over-ripe: grain very hard, cannot be dented by the thumbnail; the harvested sample was seeds).

Phenotypic variation among the lines for shoot biomass

Significant differences among the lines for shoot biomass measured at different developmental stages were tested using PROC ANOVA in the Statistical Analysis System (SAS v.9) software.

Measurement of sugars, starch and amino acids

Soluble and insoluble sugars in leaf and seeds were determined as described by Ahkami et al. (2009). Starch hydrolysis in the pellet remaining after separation of soluble and insoluble compounds was carried out by the incubation of aliquots in a buffer containing 50 ml of sodium acetate, pH 5.2 and 7 U mg^{-1} amyloglucosidase (Roche Diagnostics GmbH). The glucose produced was measured photometrically with an Elisa Reader (Bio-Tek, Synergy HT). Amino acids were analyzed essentially as described by Höller et al. (2014).

Extraction of metabolites and non-targeted and targeted metabolite profiling

Targeted metabolite analysis was performed according to Höller et al. (2014) with some modifications. Metabolites were extracted from barley leaves and seeds, each 100 mg of frozen fresh plant tissue. The extraction buffer containing 1 ml of chloroform/methanol in a ratio of 1:1 (v/v) was added. The mixture allows the extraction of lipophilic and hydrophilic substances together. Samples were mixed thoroughly and placed on a vortex at 4°C while shaking carefully for at least 20 min. A 300 µl aliquot of HPLC grade water was added to each sample and mixed carefully. Subsequently, samples were centrifuged at 14,000 r.p.m. at 4°C for 10 min and the supernatant was transferred to a new Eppendorf tube and dried in a speed vac (Christ RVC2-33IR) for 2 h at 35°C. The pellet was re-suspended in 100–200 µl of purest grade water and used immediately for the measurement of the desired compounds.

The separation and detection of metabolites was carried out using an ion chromatography system (Dionex Thermofisher) connected to a triple quadrupole mass spectrometer QQQ6490 (Agilent Technologies). Electrospray ionization-tandem mass spectrometry (ESI-MS/MS) analysis was conducted in the negative ionization mode and the following parameters were employed: desolvation temperature 250°C, nitrogen gas of 720 l h^{-1} with a heater temperature of 250°C, capillary voltage 3.5 kV and different dwell times between 40 and 200 s. The collision energy (CE) differed among the compounds and was in the range between 6 and 50 for different masses. Deprotonated ions $[M\text{-}H]^-$ were monitored with a span of 1 amu. Multiple reaction monitoring (MRM) was performed to identify individual compounds accurately. This allows minimizing parallel monitoring and enhancing the sensitivity. Pure standards for all metabolites were prepared and specific masses were determined using a MassHunter Optimizer 7.1.7109.0. Quantification of the desired compounds was performed with authentic standards at different concentrations.

Non-targeted metabolite profiling was carried out using gas chromatography–mass spectrometry (GC-TOF-MS) according to Lisec et al. (2006). The GC-MS system was composed of a GC-TOF-MS system including an A7890gas chromatograph (Agilent), a Twister XXL autoinjector (GERSTEL) and a GCT Premier TOF mass spectrometer (Waters Corporation). The mass spectrometer was tuned according to the method described by Lippmann et al. (2009), on a 30 m DB5ms capillary column (Phenomenex) with 0.25 mm inner diameter and 0.25 µm film thickness including a 5 m guard column. All chromatograms were processed after converting to netCDF format and analyzed using the web-based processing platform MeltDB (Neuweger et al. 2008). Briefly, two different tools were used: the MeltDB profiling pipeline for observation and annotation and the MeltDB warped profiling pipeline for observation of peaks. The detection of peaks in all samples was performed for high sensitivity (FWHM = 7, SN = 10) using the XCMS tool of R (Smith et al. 2006). Soluble amino acids were measured using a reversed-phase HPLC system as described by Höller et al. (2014). The concentrations of sugar alcohols were determined using an ion chromatography system (Dionex) according to Höller et al. (2014).

Extraction and measurement of the maximum enzyme activity

The extraction of enzymes was carried out according to Ding et al. (2007). The maximum enzyme activity of cytosolic, acid and cell wall invertases was assayed as described by Ahkami et al. (2009). Plastidic glyceraldehyde-3-phosphate dehydrogenase was measured in 0.1 M Tris (pH 7.0) containing 5 mM $MgCl_2$, 1 mM sodium fluoride, 5 mM dithiothreitol, 5 mM 3-phosphoglycerate (3PGA), 0.4 mM NADPH, 2 U of phosphoglycerate kinase (PGK) and protein extract. The reaction was started by adding ATP (2.5 mM final concentration), and the absorption of NADP was followed at a wavelength of 340 nm. The cytoplasmic fructose-1,6-bisphosphatase and plastidic fructose-1,6-biosphosphatase were measured according to Kelly et al. (1982). The activity of cytosolic and plastidic aldolase was measured according to Haake et al. (1998). The activity of sucrose synthase was measured with a new MS-based method in which produced UDP glucose was detected after incubation of protein extracts with the appropriate substrates. The reaction assay medium contained 100 mM HEPES-KOH (pH 7.0), 0.5 M sucrose, 20 mM UDP and 20 µl of the protein extract in a final volume of 100 µl. Samples were incubated at 30°C for 3 h. The reactions were stopped at 95°C for 5 min. Blanks were prepared with the above protocol but were heat inactivated immediately at 95°C for 5 min. The determination of UDP glucose was carried out with ion chromatography coupled to an Agilent 6490 triple quadrupole (QQQ) mass spectrometer as described above for metabolite profiling with minor modification of the gradient that was shortened to 20 min (Heinzel and Rolletschek 2011). The activity of phosphofructokinase and pyruvate kinase was determined according to Hajirezaei et al. (1993). Phosphoenolpyruvate carboxylase was assayed as previously described by Rolletschek et al. (2004). The activity of malate dehydrogenase and isocitrate dehydrogenase was measured spectrometrically by the method described previously by Jenner et al. (2001) and Gibon et al. (2004), respectively. Glucose-6-phosphate dehydrogenase was measured by the method described by Ahkami et al. (2009). The enzyme activity of 6-phosphogluconate dehydrogenase was analyzed in a reaction buffer containing 50 mM HEPES-NaOH (pH 7.2), 5 mM $MgCl_2$ and 1 mM NADP. A final concentration of 1 mM 6-phosphogluconate was used to start the reaction. The activity of PGI and PGM was measured in accordance with Hattenbach and Heineke (1999). The activity of ADP-glucose pyrophosphorylase was measured spectrometrically by monitoring NADH production at 340 nm. The reaction buffer contained 100 mM HEPES-KOH (pH 7.8), 2 mM ADP glucose, 5 mM $MgCl_2$, 0.5 mM NAD, 2 U of PGM and 5 U of glucose-6-phosphate dehydrogenase. The reaction was started by adding of 2 mM sodium pyrophosphate (PPi). Alanine aminotransferase and aspartate aminotransferase were measured as described by Holtum and Winter (1982). Glutamine oxoglutarate aminotransferase was measured in a reaction mixture containing 50 mM Tris–HCl (pH 7.9), 40 mM sorbitol (Sbt), 5 mM 2-oxoglutarate, 5 mM glutamine, 10 mM glucose-6-phosphate and 50 µl of fresh protein extract. Samples were incubated at 30°C for 3 h and stopped at 95°C for 5 min. Blanks containing buffer and protein extract were inactivated immediately at 95°C for 10 min. The determination of produced glutamate was performed by reversed phase HPLC using on a C18 column as described by Rolletschek et al. (2002).

Transcriptome analysis

Total RNA was extracted from 200 mg of leaves and seeds of the same material that was used for metabolite and enzyme measurements using TRIzol reagent (Invitrogen) following the manufacturer's protocols. RNA was purified using the RNasey Min Elute cleanup kit (Qiagen). The quality of total RNA was checked before starting the hybridization process on an Agilent BioAnalyzer 2100 (Agilent Technology). A custom barley Agilent microarray technology containing approximately 56,000 genes has been created (in a 60K × 8 plex format), which cover a broad range of metabolic and growth developmental processes. Three biological replicates of flag leaves and seed tissues were used to synthesize amplified cDNA (Quick Amp Labeling Kit, Agilent). The detailed procedures of labeling, hybridization and scanning of Agilent Barley GeneChips were performed according to Koppolu et al. (2013). The microarray TIF images were processed to run batch extractions by choosing an appropriate grid using Agilent's Feature Extraction Software version 11.0. The quantified feature text file is first analyzed for quality checks using the Agilent QC chart tool. The gene expression data of 56K genes from the experiments which passed quality control were subjected to quantile normalization (Wu et al. 2004). Fold differences calculated between HOR216 vs. S42IL107 flag leaf samples were used as differentially expressed gene sets. A similar comparison was made for seed samples. The one-way analysis of variation which applied a Benjamini–Hochberg ($P \leq 0.05$) for correction of the P-value was used to assign significant differences in the expression levels (Benjamini and Hochberg 1995). Functional categorization by using Gene Ontology (GO) terms was performed as previously described using VANTED, a tool for the visualization and analysis of networks with related experimental data (Junker et al. 2006). The R-values for significant over-representation of a particular GO category were calculated using one of VANTED's main modules using Fisher's exact test.

Visualization of transcriptome data onto metabolic pathways using Mapman

The 34 MapMan BINs/subBINS used for the Arabidopsis, which have been adapted previously to the most similar Arabidopsis genes by Sreenivasulu et al. (2008), was used for the visualization of transcriptome results within the current study. The data including differentially expressed genes between genotypes were imported into MapMan and mapped onto diagrams of metabolic pathway and visualized as false color code rectangles. MapMan version 3.05, which is freely available at http://mapman.gabipd.org, was employed.

Graphical visualization and network correlation analysis

All graphs and heat maps were drawn using Microsoft PowerPoint and Excel (Microsoft Office 2007). Network correlation analyses were performed by calculating all pairwise correlations for metabolites, enzyme activities, transcripts and phenotypical parameters and their combinations in different tissues and at various developmental stages of barley using VANTED (Junker et al. 2006). VANTED was also used for constructing and modifying pathways from the KEGG database or MetaCrop (Grafahrend-Belau et al. 2008). The pathways of central metabolism were mapped with the results of correlations among metabolic traits and between metabolic traits and biomass.

Supplementary data

Supplementary data are available at PCP online.

Funding

This work received funding from The Ministry of Education and Research (BMBF) of Germany.

Acknowledgments

We would like to thank Wally Wendt, Melanie Ruff, Heike Nierig and Mandy Pueffeld for their excellent technical assistance. We are indebted to Enk Geyer and his colleagues for preparation and taking care of greenhouse and field plants. All experiments were conducted at the Leibniz institute of Plant Genetics and Crop Plant Research in Gatersleben, Germany.

Disclosures

The authors have no conflicts of interest to declare.

References

Aharoni, A. and Brandizzi, F. (2012) High-resolution measurements in plant biology. *Plant J.* 70: 1–4.

Ahkami, A.H., Lischewski, S., Haensch, K.T., Porfirova, S., Hofmann, J., Rolletschek, H., et al. (2009) Molecular physiology of adventitious root formation in Petunia hybrida cuttings: involvement of wound response and primary metabolism. *New Phytol.* 181: 613–625.

Beatty, P.H., Shrawat, A.K., Carroll, R.T., Zhu, T. and Good, A.G. (2009) Transcriptome analysis of nitrogen-efficient rice over-expressing alanine aminotransferase. *Plant Biotechnol. J.* 7: 562–576.

Benjamini, Y. and Hochberg, Y. (1995) Controlling the false discovery rate: a practical and powerful approach to multiple testing. *J. R. Stat. Soc. Ser. B: Stat. Methodol.* 57: 289–300.

Bihmidine, S., Hunter, C.T., III, Johns, C.E., Koch, K.E. and Braun, D.M. (2013) Regulation of assimilate import into sink organs: update on molecular drivers of sink strength. *Front. Plant. Sci.* 4: 177.

Bollina, V., Kushalappa, A.C., Choo, T.M., Dion, Y. and Rioux, S. (2011) Identification of metabolites related to mechanisms of resistance in barley against Fusarium graminearum, based on mass spectrometry. *Plant Mol. Biol.* 77: 355–370.

Borisjuk, L., Rolletschek, H., Radchuk, R., Weschke, W., Wobus, U. and Weber, H. (2004) Seed development and differentiation: a role for metabolic regulation. *Plant Biol.* 6: 375–386.

Burton, R.A. and Fincher, G.B. (2014) Plant cell wall engineering: applications in biofuel production and improved human health. *Curr. Opin. Biotechnol.* 26: 79–84.

Carrari, F., Baxter, C., Usadel, B., Urbanczyk-Wochniak, E., Zanor, M.-I., Nunes-Nesi, A., et al. (2006) Integrated analysis of metabolite and transcript levels reveals the metabolic shifts that underlie tomato fruit development and highlight regulatory aspects of metabolic network behavior. *Plant Physiol.* 142: 1380–1396.

Cho, M.-H., Jang, A., Bhoo, S.H., Jeon, J.-S. and Hahn, T.-R. (2012) Manipulation of triose phosphate/phosphate translocator and cytosolic fructose-1, 6-bisphosphatase, the key components in photosynthetic sucrose synthesis, enhances the source capacity of transgenic Arabidopsis plants. *Photosynth. Res.* 111: 261–268.

Coleman, H.D., Beamish, L., Reid, A., Park, J.-Y. and Mansfield, S.D. (2010) Altered sucrose metabolism impacts plant biomass production and flower development. *Transgenic Res.* 19: 269–283.

Coleman, H.D., Yan, J. and Mansfield, S.D. (2009) Sucrose synthase affects carbon partitioning to increase cellulose production and altered cell wall ultrastructure. *Proc. Natl Acad. Sci. USA* 106: 13118–13123.

Covington, M.F., Maloof, J.N., Straume, M., Kay, S.A. and Harmer, S.L. (2008) Global transcriptome analysis reveals circadian regulation of key pathways in plant growth and development. *Genome Biol.* 9: R130.

Dai, Z.W., Léon, C., Feil, R., Lunn, J.E., Delrot, S. and Gomès, E. (2013) Metabolic profiling reveals coordinated switches in primary carbohydrate metabolism in grape berry (Vitis vinifera L.), a non-climacteric fleshy fruit. *J. Exp. Bot.* 64: 1345–1355.

De Silva, J., Arrowsmith, D., Hellyer, A., Whiteman, S. and Robinson, S. (1994) Xyloglucan endotransglycosylase and plant growth. *J. Exp. Bot.* 45: 1693–1701.

Ding, L., Hofius, D., Hajirezaei, M.-R., Fernie, A.R., Börnke, F. and Sonnewald, U. (2007) Functional analysis of the essential bifunctional tobacco enzyme 3-dehydroquinate dehydratase/shikimate dehydrogenase in transgenic tobacco plants. *J. Exp. Bot.* 58: 2053–2067.

Fernie, A.R. and Schauer, N. (2009) Metabolomics-assisted breeding: a viable option for crop improvement? *Trends Genet.* 25: 39–48.

Fincher, G.B. (2009) Revolutionary times in our understanding of cell wall biosynthesis and remodeling in the grasses. *Plant Physiol.* 149: 27–37.

Gibon, Y., Blaesing, O.E., Hannemann, J., Carillo, P., Höhne, M., Hendriks, J.H.M., et al. (2004) A robot-based platform to measure multiple enzyme activities in Arabidopsis using a set of cycling assays: comparison of changes of enzyme activities and transcript levels during diurnal cycles and in prolonged darkness. *Plant Cell* 16: 3304–3325.

Gordon, A., Ryle, G. and Webb, G. (1980) The relationship between sucrose and starch during 'dark'export from leaves of uniculm barley. *J. Exp. Bot.* 31: 845–850.

Grafahrend-Belau, E., Weise, S., Koschützki, D., Scholz, U., Junker, B.H. and Schreiber, F. (2008) MetaCrop: a detailed database of crop plant metabolism. *Nucleic Acids Res.* 36: D954–D958.

Haake, V., Zrenner, R., Sonnewald, U. and Stitt, M. (1998) A moderate decrease of plastid aldolase activity inhibits photosynthesis, alters the levels of sugars and starch, and inhibits growth of potato plants. *Plant J.* 14: 147–157.

Hajirezaei, M., Sonnewald, U., Viola, R., Carlisle, S., Dennis, D. and Stitt, M. (1993) Transgenic potato plants with strongly decreased expression of pyrophosphate:fructose-6-phosphate phosphotransferase show no visible phenotype and only minor changes in metabolic fluxes in their tubers. *Planta* 192: 16–30.

Harrison, E.P., Willingham, N.M., Lloyd, J.C. and Raines, C.A. (1997) Reduced sedoheptulose-1, 7-bisphosphatase levels in transgenic tobacco lead to decreased photosynthetic capacity and altered carbohydrate accumulation. *Planta* 204: 27–36.

Hattenbach, A. and Heineke, D. (1999) On the role of chloroplastic phosphoglucomutase in the regulation of starch turnover. *Planta* 207: 527–532.

Heinzel, N. and Rolletschek, H. (2011) Primary metabolite analysis of plant material using a triple quadrupole MS coupled to a monolith anion-exchange column. Dionex, Customer Application Note.

Hennen-Bierwagen, T.A., Myers, A.M. and Becraft, P. (2013) Genomic specification of starch biosynthesis in maize endosperm. *In* Seed Genomics. Edited by Becraft P.W.. pp. 123–137. Wiley-Blackwell, Oxford.

Hertzberg, M., Aspeborg, H., Schrader, J., Andersson, A., Erlandsson, R., Blomqvist, K., et al. (2001) A transcriptional roadmap to wood formation. *Proc. Natl Acad. Sci. USA* 98: 14732–14737.

Hill, C.B., Taylor, J.D., Edwards, J., Mather, D., Bacic, A., Langridge, P., et al. (2013) Whole-genome mapping of agronomic and metabolic traits to identify novel quantitative trait loci in bread wheat grown in a water-limited environment. *Plant Physiol.* 162: 1266–1281.

Höller, S., Hajirezaei, M.R., von Wirén, N. and Frei, M. (2014) Ascorbate metabolism in rice genotypes differing in zinc efficiency. *Planta* 239: 367–379.

Holtum, J.A. and Winter, K. (1982) Activity of enzymes of carbon metabolism during the induction of Crassulacean acid metabolism in Mesembryanthemum crystallinum L. *Planta* 155: 8–16.

Jenner, H.L., Winning, B.M., Millar, A.H., Tomlinson, K.L., Leaver, C.J. and Hill, S.A. (2001) NAD malic enzyme and the control of carbohydrate metabolism in potato tubers. *Plant Physiol.* 126: 1139–1149.

Junker, B., Klukas, C. and Schreiber, F. (2006) VANTED: a system for advanced data analysis and visualization in the context of biological networks. *BMC Bioinformatics* 7: 109.

Kacser, H.A. and Burns, J. (1973) The control of flux. *Symp. Soc. Exp. Biol.* 27: 65–104.

Kelly, G.J., Zimmermann, G. and Latzko, E. (1982) Fructose-bisphosphatase from spinach leaf chloroplast and cytoplasm. *Methods Enzymol.* 90: 371–378.

Keurentjes, J.J.B., Sulpice, R., Gibon, Y., Steinhauser, M.C., Fu, J., Koornneef, M., et al. (2008) Integrative analyses of genetic variation in enzyme activities of primary carbohydrate metabolism reveal distinct modes of regulation in Arabidopsis thaliana. *Genome Biol.* 9: R129.

Kirst, M., Myburg, A.A., De León, J.P., Kirst, M.E., Scott, J. and Sederoff, R. (2004) Coordinated genetic regulation of growth and lignin revealed by quantitative trait locus analysis of cDNA microarray data in an interspecific backcross of eucalyptus. *Plant Physiol.* 135: 2368–2378.

Koppolu, R., Anwar, N., Sakuma, S., Tagiri, A., Lundqvist, U., Pourkheirandish, M., et al. (2013) Six-rowed spike4 (Vrs4) controls

spikelet determinacy and row-type in barley. *Proc. Natl Acad. Sci. USA* 110: 13198–13203.

Lancashire, P., Bleiholder, H., Boom, T., Langelüddeke, P., Stauss, R., Weber, E., et al. (1991) A uniform decimal code for growth stages of crops and weeds. *Ann. Appl. Biol.* 119: 561–601.

Lawlor, D.W. (2002) Carbon and nitrogen assimilation in relation to yield: mechanisms are the key to understanding production systems. *J. Exp. Bot.* 53: 773–787.

Lippmann, R., Kaspar, S., Rutten, T., Melzer, M., Kumlehn, J., Matros, A., et al. (2009) Protein and metabolite analysis reveals permanent induction of stress defense and cell regeneration processes in a tobacco cell suspension culture. *Int. J. Mol. Sci.* 10: 3012–3032.

Lisec, J., Meyer, R.C., Steinfath, M., Redestig, H., Becher, M., Witucka-Wall, H., et al. (2008) Identification of metabolic and biomass QTL in Arabidopsis thaliana in a parallel analysis of RIL and IL populations. *Plant J.* 53: 960–972.

Lisec, J., Schauer, N., Kopka, J., Willmitzer, L. and Fernie, A.R. (2006) Gas chromatography–mass spectrometry-based metabolite profiling in plants. *Nat. Protoc.* 1: 387–396.

Lloyd, J.R. and Kossmann, J. (2015) Transitory and storage starch metabolism: two sides of the same coin? *Curr. Opin. Biotechnol.* 32: 143–148.

McLaren, J.S. (2005) Crop biotechnology provides an opportunity to develop a sustainable future. *Trends Biotechnol.* 23: 339–342.

Meyer, R.C., Steinfath, M., Lisec, J., Becher, M., Witucka-Wall, H., Törjék, O., et al. (2007) The metabolic signature related to high plant growth rate in Arabidopsis thaliana. *Proc. Natl Acad. Sci. USA* 104: 4759–4764.

Micallef, B.J., Haskins, K.A., Vanderveer, P.J., Roh, K.-S., Shewmaker, C.K. and Sharkey, T.D. (1995) Altered photosynthesis, flowering, and fruiting in transgenic tomato plants that have an increased capacity for sucrose synthesis. *Planta* 196: 327–334.

Miyagawa, Y., Tamoi, M. and Shigeoka, S. (2001) Overexpression of a cyanobacterial fructose-1, 6-/sedoheptulose-1, 7-bisphosphatase in tobacco enhances photosynthesis and growth. *Nat. Biotechnol.* 19: 965–969.

Neuweger, H., Albaum, S.P., Dondrup, M., Persicke, M., Watt, T., Niehaus, K., et al. (2008) MeltDB: a software platform for the analysis and integration of metabolomics experiment data. *Bioinformatics* 24: 2726–2732.

Nishitani, K. (1997) The role of endoxyloglucan transferase in the organization of plant cell walls. *Int. Rev. Cytol.* 173: 157–206.

O'Hara, L.E., Paul, M.J. and Wingler, A. (2012) How do sugars regulate plant growth and development? New insight into the role of trehalose-6-phosphate. *Mol. Plant* 6: 261–274.

Orzechowski, S. (2008) Starch metabolism in leaves. *Acta Biochim. Pol.* 55: 435–445.

Paul, M.J., Primavesi, L.F., Jhurreea, D. and Zhang, Y. (2008) Trehalose metabolism and signaling. *Annu. Rev. Plant Biol.* 59: 417–441.

Pollock, C. and Cairns, A. (1991) Fructan metabolism in grasses and cereals. *Annu. Rev. Plant Biol.* 42: 77–101.

Ridley, M. (2010) Nitrogen-use efficiency, the next green revolution. The Economist, The World in 2010.

Riedelsheimer, C., Lisec, J., Czedik-Eysenberg, A., Sulpice, R., Flis, A., Grieder, C., et al. (2012) Genome-wide association mapping of leaf metabolic profiles for dissecting complex traits in maize. *Proc. Natl Acad. Sci. USA* 109: 8872–8877.

Rolletschek, H., Borisjuk, L., Radchuk, R., Miranda, M., Heim, U., Wobus, U., et al. (2004) Seed-specific expression of a bacterial phosphoenolpyruvate carboxylase in Vicia narbonensis increases protein content and improves carbon economy. *Plant Biotechnol. J.* 2: 211–219.

Rolletschek, H., Hajirezaei, M.-R., Wobus, U. and Weber, H. (2002) Antisense-inhibition of ADP-glucose pyrophosphorylase in Vicia narbonensis seeds increases soluble sugars and leads to higher water and nitrogen uptake. *Planta* 214: 954–964.

Schluepmann, H., van Dijken, A., Aghdasi, M., Wobbes, B., Paul, M. and Smeekens, S. (2004) Trehalose mediated growth inhibition of Arabidopsis seedlings is due to trehalose-6-phosphate accumulation. *Plant Physiol.* 135: 879–890.

Sharkey, T.D., Savitch, L.V., Vanderveer, P.J. and Micallef, B.J. (1992) Carbon partitioning in a Flaveria linearis mutant with reduced cytosolic fructose bisphosphatase. *Plant Physiol.* 100: 210–215.

Sicher, R.C. and Kremer, D.F. (1984) Changes of sucrose-phosphate synthase activity in barley primary leaves during light/dark transitions. *Plant Physiol.* 76: 910–912.

Smith, C.A., Want, E.J., O'Maille, G., Abagyan, R. and Siuzdak, G. (2006) XCMS: processing mass spectrometry data for metabolite profiling using nonlinear peak alignment, matching, and identification. *Anal. Chem.* 78: 779–787.

Sreenivasulu, N., Usadel, B., Winter, A., Radchuk, V., Scholz, U., Stein, N., et al. (2008) Barley grain maturation and germination: metabolic pathway and regulatory network commonalities and differences highlighted by new MapMan/PageMan profiling tools. *Plant Physiol.* 146: 1738–1758.

Sreenivasulu, N. and Wobus, U. (2013) Seed-development programs: a systems biology-based comparison between dicots and monocots. *Annu. Rev. Plant Biol.* 64: 189–217.

Steinhauser, M.-C., Steinhauser, D., Koehl, K., Carrari, F., Gibon, Y., Fernie, A.R., et al. (2010) Enzyme activity profiles during fruit development in tomato cultivars and Solanum pennellii. *Plant Physiol.* 153: 80–98.

Stettler, M., Eicke, S., Mettler, T., Messerli, G., Hörtensteiner, S. and Zeeman, S.C. (2009) Blocking the metabolism of starch breakdown products in Arabidopsis leaves triggers chloroplast degradation. *Mol. Plant* 2: 1233–1246.

Stitt, M., Müller, C., Matt, P., Gibon, Y., Carillo, P., Morcuende, R., et al. (2002) Steps towards an integrated view of nitrogen metabolism. *J. Exp. Bot.* 53: 959–970.

Stitt, M. and Zeeman, S.C. (2012) Starch turnover: pathways, regulation and role in growth. *Curr. Opin. Plant Biol.* 15: 282–292.

Streb, S. and Zeeman, S.C. (2012) Starch metabolism in Arabidopsis. *Arabidopsis Book* 10: e0160.

Sulpice, R., Nikoloski, Z., Tschoep, H., Antonio, C., Kleessen, S., Larhlimi, A., et al. (2013) Impact of the carbon and nitrogen supply on relationships and connectivity between metabolism and biomass in a broad panel of Arabidopsis accessions. *Plant Physiol.* 162: 347–363.

Sulpice, R., Pyl, E.-T., Ishihara, H., Trenkamp, S., Steinfath, M., Witucka-Wall, H., et al. (2009) Starch as a major integrator in the regulation of plant growth. *Proc. Natl Acad. Sci. USA* 106: 10348–10353.

Sulpice, R., Trenkamp, S., Steinfath, M., Usadel, B., Gibon, Y., Witucka-Wall, H., et al. (2010) Network analysis of enzyme activities and metabolite levels and their relationship to biomass in a large panel of Arabidopsis accessions. *Plant Cell* 22: 2872–2893.

Tang, G.-Q. and Sturm, A. (1999) Antisense repression of sucrose synthase in carrot (Daucus carota L.) affects growth rather than sucrose partitioning. *Plant Mol. Biol.* 41: 465–479.

Wen, W., Li, K., Alseekh, S., Omranian, N., Zhao, L., Zhou, Y., et al. (2015) Genetic determinants of the network of primary metabolism and their relationships to plant performance in a maize recombinant inbred line population. *Plant Cell* 27: 1839–1856.

Wingler, A., Fritzius, T., Wiemken, A., Boller, T. and Aeschbacher, R.A. (2000) Trehalose induces the ADP-glucose pyrophosphorylase gene, ApL3, and starch synthesis in Arabidopsis. *Plant Physiol.* 124: 105–114.

Wu, Z., Irizarry, R.A., Gen tleman, R., Martinez-Murillo, F. and Spencer, F. (2004) A model-based background adjustment for oligonucleotide expression arrays. *J. Amer. Stat. Assoc.* 99: 909–917.

Xu, S.-M., Brill, E., Llewellyn, D.J., Furbank, R.T. and Ruan, Y.-L. (2011) Overexpression of a potato sucrose synthase gene in cotton accelerates leaf expansion, reduces seed abortion, and enhances fiber production. *Mol. Plant* 5: 430–431.

Xue, G.-P., McIntyre, C.L., Jenkins, C.L., Glassop, D., van Herwaarden, A.F. and Shorter, R. (2008) Molecular dissection of variation in carbohydrate

metabolism related to water-soluble carbohydrate accumulation in stems of wheat. *Plant Physiol.* 146: 441–454.

Yamaya, T., Obara, M., Nakajima, H., Sasaki, S., Hayakawa, T. and Sato, T. (2002) Genetic manipulation and quantitative trait loci mapping for nitrogen recycling in rice. *J. Exp. Bot.* 53: 917–925.

Zhang, N., Gibon, Y., Gur, A., Chen, C., Lepak, N., Höhne, M., et al. (2010) Fine quantitative trait loci mapping of carbon and nitrogen metabolism enzyme activities and seedling biomass in the maize IBM mapping population. *Plant Physiol.* 154: 1753–1765.

Zhu, X.-G., de Sturler, E. and Long, S.P. (2007) Optimizing the distribution of resources between enzymes of carbon metabolism can dramatically increase photosynthetic rate: a numerical simulation using an evolutionary algorithm. *Plant Physiol.* 145: 513–526.

Zrenner, R., Salanoubat, M., Willmitzer, L. and Sonnewald, U. (1995) Evidence of the crucial role of sucrose synthase for sink strength using transgenic potato plants (Solanum tuberosum L.). *Plant J.* 7: 97–107.